A Retrospective on the 1999 Microwave Pioneer Award

Robert L. Eisenhart, *Fellow, IEEE*

(Invited Paper)

***Abstract*— This retrospective looks back at Eisenhart and Khan's paper, which was the basis for selection of the 1999 Microwave Pioneer Award. The subject is the waveguide circuit commonly referred to as a "post in a waveguide." Here is the story about that paper, where it started, what it contributed, and its impact over the last 28 years.**

***Index Terms*—Analysis, equivalent circuit, measurement, post, waveguide mount.**

I. Preface

"POST in a waveguide" is an oversimplified, but common description of an often used waveguide circuit, and is the subject of [1]. This paper became the basis for the 1999 Microwave Pioneer Award.

> I believe that this is the single most important paper that has been published in the MTT Transactions on microwave waveguides. The paper made it possible to predict the embedding impedances of diode mixers and oscillators in waveguides over a wide range of frequencies, including harmonics. Previously, adjustments were done empirically, and they were quite difficult because of the complicated behavior of the impedances at different harmonics. In addition, the work gave a clear physical picture of what determined the impedance. The propagating modes contribute to the real part, the cut-off modes to the reactive part, and the shape and structure of the post gave the coupling coefficients to the modes. Finally, the measurements that accompanied the theory were so beautifully done that even though the behavior of the impedances was surprising, there was simply no doubt that Eisenhart and Khan had solved the problem completely.
>
> Prof. David B. Rutledge, Guest Editor
> Electrical Engineering Department
> California Institute of Technology
> Pasadena, CA, USA

II. Problem Description

In the theoretical analysis of oscillators, parametric amplifiers, and frequency converters, i.e., active circuits, general impedance functions $Z(f)$ are assumed to be known and are utilized accordingly as parameters when determining such quantities as power, frequency, gain, bandwidth, stability and noise figure. In a practical sense, this impedance for a microwave circuit, as shown in Fig. 1, was not available for design purposes. Determination of the impedance seen by the device becomes very difficult due to the complex nature of the configuration. In fact, the accepted view was that the post in a waveguide structure was electromagnetically too complex to permit accurate modeling, and measurement techniques too primitive to permit reliable verification. Design of real subsystems was done on a experience–experimental trial-and-error basis. The question then was asked, "why use such a complex structure?" The answer came from experimental work that showed this circuit worked well for many applications because there is strong coupling between the "post" current and propagated energy within the waveguide.

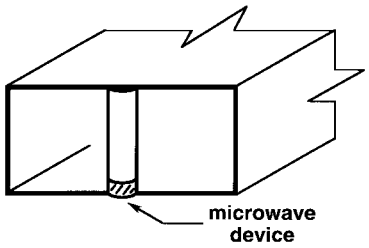

Fig. 1. Typical mount configuration with the device mounted at the bottom of the waveguide.

Therefore, the objective was to characterize the impedance of the microwave mount (shown in Fig. 1) commonly used for connecting small microwave devices in shunt across a waveguide. The term "impedance characterization" implies complete knowledge of the driving point and transfer impedances associated with and between each and every entry or terminal port of the mount. Once such a circuit is established, standard circuit analysis techniques can be applied to design the mount.

III. Analytical Development

In 1966 and 1967, Getsinger suggested a relatively simple equivalent circuit for the waveguide mount [2], [3]. A more complete description was discussed by Yamashita and Baird [4] who used the variational approach to solve for the impedance by considering the post as a radiating antenna element. They developed an equivalent circuit that helped them analyze the operation of a tunnel diode oscillator.

Manuscript received March 26, 1999.

The author is with Eisenhart & Associates, Woodland Hills, CA 91367 USA (e-mail: r.l.eisenhart@ieee.org).

Publisher Item Identifier S 0018-9480(99)08410-0.

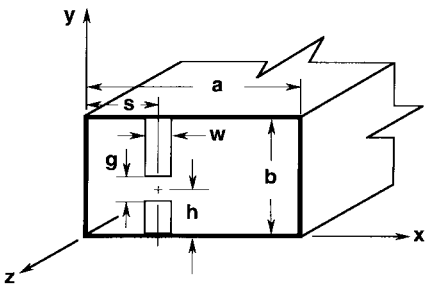

Fig. 2. Description of mount parameters.

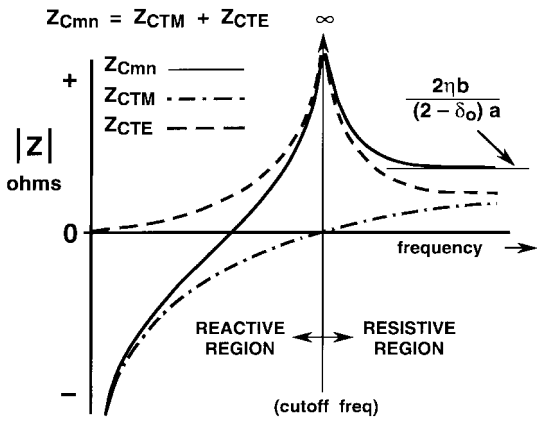

Fig. 3. Mode pair impedance plot.

Yamashita and Baird provided the starting point for the subject analysis, which was then extended, based upon the induced EMF method of Carter [5]. The following five-step procedure was set up [1] to analyze "the post in a waveguide" circuit.

Step 1: Determine the dyadic Green's function for the waveguide.

Step 2: Express the post current in a general set of orthogonal functions.

Step 3: Determine an expression for the electric field anywhere within the waveguide.

Step 4: Develop an expression for the electric field at the gap using the Lorentz reciprocity theorem.

Step 5: Put the related expansion terms in the form of power equations and interpret as equivalent-circuit elements.

A simplifying approximation was to use a strip or flat post to represent a circular post [4] with the flat post width equal to 1.8 circular post diameter. The key deviation from [4] was the use of a general Fourier series in Step 2, eliminating the assumption about the post current function. It was thought (correctly) that the impedance should be determined only by the configuration and not dependent on the actual current. After much mathematical manipulation it became possible to show that the current function canceled out and only the dimensions of the structure were independent parameters. That was the first big breakthrough.

Although complex mathematics were used to develop the circuit element values, understanding of those mathematics is not necessary to appreciate and make use of the symmetries and simplicity of the resulting equivalent-circuit configuration. Previous modeling attempts were incomplete or incorrect and never accurately predicted the desired impedance. The range of mount parameters and/or frequency were restricted. Usually the post was located in the center of the waveguide, and the device positioned at the bottom of the guide, as in Fig. 1. In addition, the waveguide height was often reduced for matching purposes, and the frequency range restricted to that of the dominant mode. All of these restrictions were removed in the present analysis. The remaining restrictions relate to the size and shape of the post and gap, and do not significantly limit the applicability of the analysis since conventional diode dimensions fall easily within acceptable ranges.

All of the mount configuration parameters, shown in Fig. 2, are variables and the significance of each parameter is determined in the resulting characterization. All evanescent and propagating modes are included in the analysis. This provides considerable generality in the design of circuits. The modeling was sufficiently precise to be useful at frequencies well above the fundamental-mode band, describing harmonic circuit loading as well.

In addition to Yamashita and Baird, other "shoulders" that deserve mentioning include the following:

1) Getsinger—approach to equivalent circuits;
2) Tai—guru of Green's functions and Doctoral Committee member;
3) Collin—Lorentz Reciprocity Theorem in [6];
4) Fourier—thanks for the series representation;
5) Carter—thanks for the induced EMF method.

A technical report [7] documenting the work for the research sponsor is a more complete development than what is in [1].

IV. Equivalent-Circuit Representation

The equivalent circuit takes into account the effect of a doubly infinite number of waveguide modes, all connected together. Two issues are: 1) what are the broad-band characteristics of the waveguide modes and 2) how do they couple together. Fig. 3 answers the first issue; it shows the form of the TE and TM mode impedances over the full frequency range from zero to infinity. As shown, modes with like indexes sum to an unusual characteristic, designated as Z_{cmn}. This is capacitive at low frequencies, goes through a zero becoming inductive up to a pole at cutoff. It then becomes resistive, representing a propagating mode carrying energy away. Each m, n pair creates one set over frequency, referred to as a mode pair.

The second issue is addressed in Fig. 4 which shows how the modes are coupled together. This coupling is really simpler than it looks because the transformers are just scaling elements. They set the coupling coefficients between the modes and the rest of the circuit. The "Gap" terminals, which is the input to the circuit that a diode sees, is at the upper left. The Z_G shown is the impedance that terminates the gap if one looks in from one of the waveguide ports, effectively reversing the input and load.

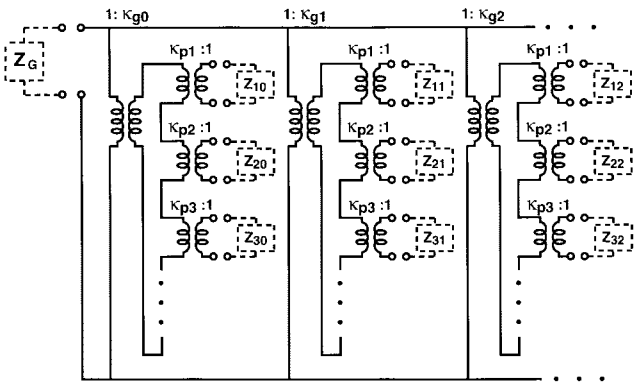

Fig. 4. Equivalent circuit of the post mount.

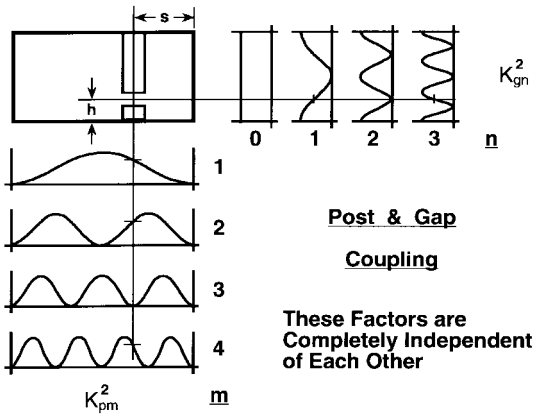

Fig. 5. Graphical description of how the mode coupling is determined.

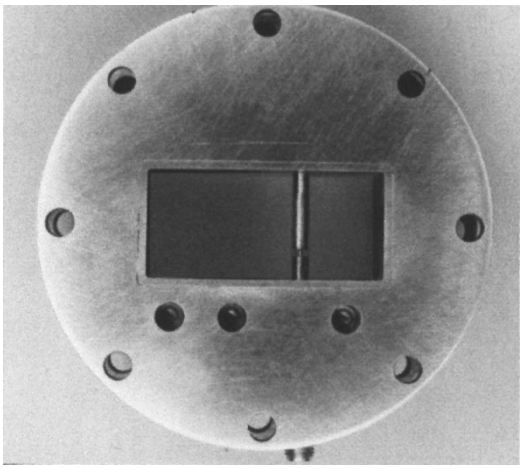

Fig. 6. C-band test fixture.

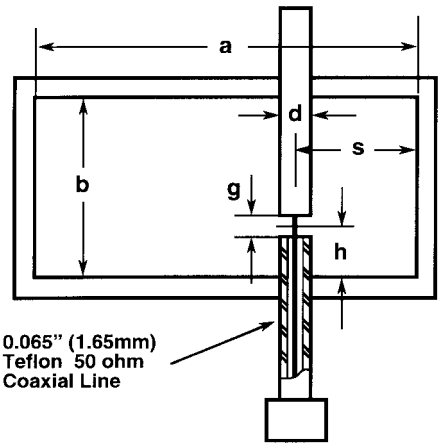

Fig. 7. Versatile measurement mount.

There are two separate coupling mechanisms for the transformers, each made up by two factors. The first factor in each case is the positional factor. Fig. 5 shows conceptually how the positional factors are determined for an arbitrarily placed gap and flat post in the waveguide cross section. Note, for example, the "n" index at the upper right. The four values for n are the labels for four mode field variations for the respective modes. The horizontal line through the middle of the gap (at $\text{height} = h$) marks a value from 0 to 1 for each of the four modes, defining the "n" positional factor. This factor is simply a function of where the gap is in the post and is called the "gap coupling factor."

A corresponding "post coupling factor" is related to the position of the flat post with respect to the waveguide sidewalls. Again note the various coupling values indicated with the vertical line for the different "m" mode indexes. This process holds for the infinite number of modes for both m and n.

The second factor in both coupling relationships is a convergence factor that simply determines how many modes should be included for both m and n indexes. These factors are related to the gap size (gap coupling) and post width (post coupling). (Note: modes for $m = 0$ do not exist.)

The equivalent circuit of Fig. 4 simply provides a means of defining the coupling between the impedance present in the gap and the mode impedances present in the waveguide arms. It is a linear passive reciprocal doubly infinite network whose elements are a function only of the mount parameters shown in Fig. 2. A summary of the mount parameter primary effects shows the following:

- a waveguide width—sets dominant mode frequency range;
- b waveguide height—multiple effects on mode characteristics;
- h gap position—gap coupling coefficients;
- s post position—post coupling coefficients;
- g gap size—sets "n" index convergence;
- w flat post width—sets "m" index convergence.

V. Experimental Development

Experimental analysis was carried out to guide and verify the theoretical work. Measurement of this terminal impedance was not considered possible because of the inaccessibility of the terminals. This fact probably accounted for the lack of published material dealing with the problem. However, with the advent of subminiature coaxial cable and connectors, it was possible to isolate the terminals electrically without affecting the surrounding field conditions by running the measurement circuit cable inside a circular post. A versatile mount fixture, shown in Fig. 6, was designed incorporating this concept to allow impedance measurements for different gap position "h" and post position "s," shown in Fig. 7. This simple approach

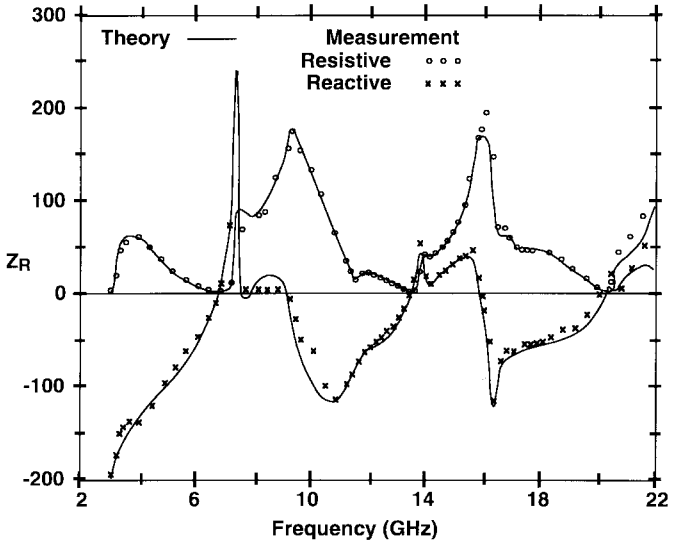

(a)

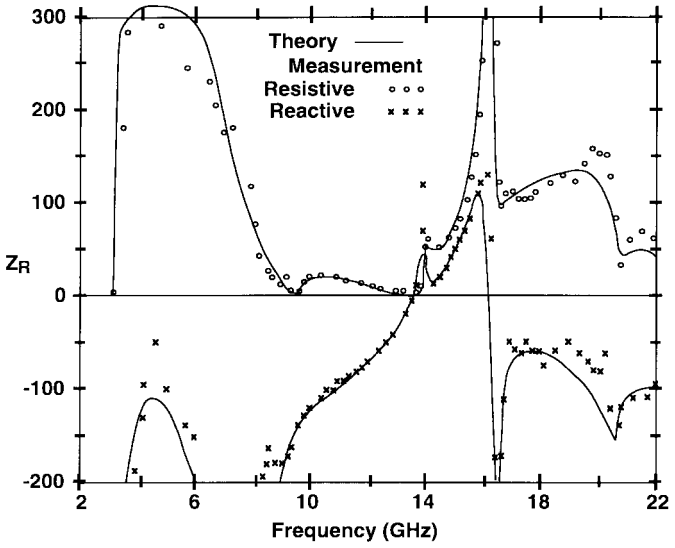

(b)

Fig. 8. Theoretical and experimental impedance comparison for different configurations of the mount. (a) $s' = 0.5$, $h' = 0.035$. (b) $s' = 0.5$, $h' = 0.5$.

of the cable in the post was a second big breakthrough. If the experimental effort had not produced such reliable and self-consistent results, the necessary insight to develop the theory would never have been obtained.

More specifically, the data indicated that the doubly infinite waveguide modes should be combined as a sum of an inverted sum, rather than as a double sum. This was a significant deviation from prevailing approaches [4].

This C-band test fixture (fundamental mode @ 4–6 GHz.) was built and used for characterization up to 22 GHz. where many higher order modes are propagating. A small 0.065-in-diameter coaxial cable was put inside the post to measure the mount as a terminating load. Measurements are shown for a range of mount parameter values. Fig. 8(a) shows the impedance for the most typical mounting configuration, where the post is centered and the gap is at the bottom. Fig. 8(b) shows the result of moving the gap halfway up the post. Since the post is centered, only coupling to the m odd modes exist. One of these, the TE_{30}, has a pole at 9.45 GHz, which causes the resistive part to have a zero at that frequency by decoupling energy to the TE_{10} propagating mode. Additional test configurations are included in [1].

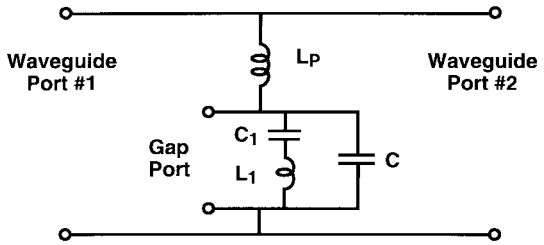

Fig. 9. Post circuit for incident TE_{10}.

The two graphs of Fig. 8 show a high degree of correlation between the theoretical results and the measured data. Based on all of the data taken, it was reasonable to conclude that the theory presented was valid and that the measurement technique developed was highly successful. Since the measurement technique had proven itself, it could be used in applications where the configuration could not be handled theoretically, thus providing a unique capability.

The experimental part provided an instrumentation technique to measure Z_R inside the waveguide, providing confirmation of the equivalent circuit (analysis). This technique has also been independently applied to a variety of structures where an internal terminal impedance characterization is desired.

VI. Post as an Obstacle

The terminals of Fig. 4 associated with the propagating modes can be considered as input ports for each respective mode, thus allowing description of the mount as a load to an incident waveguide mode. The case of the incident fundamental TE_{10} mode deserved special attention. Fig. 4 can be "turned inside-out" to result in Fig. 9, which has the TE_{10} terminals as the two waveguide ports. For this restricted frequency band, all of the other modes can be consolidated into one of the following four reactive elements.

- L_P the sum of the rest of the $n = 0$ modes.
- $C1$ capacitance due to TMm1 modes.
- $L1$ inductance due to TEm1 modes.
- C combined capacitance effect of all TE and TM modes for $n > 1$.

Some related measurements were made using standard techniques for the TE_{10} mode. An interesting case is that of the "tuned post" represented by the family of curves in Fig. 10. The gap size is varied from zero to slightly larger than 1/4 the guide height. The gap impedance Z_G is determined simply from the parallel-plate capacitance of the end of the circular post, which was centered to decouple the TE_{20} mode. This extended the dominant mode region to 7.46 GHz, the cutoff frequency for the TE_{11} and TM_{11} modes, thus permitting observation of the characteristic at 6.77 GHz where the reactance is independent of the gap size. Actually, the

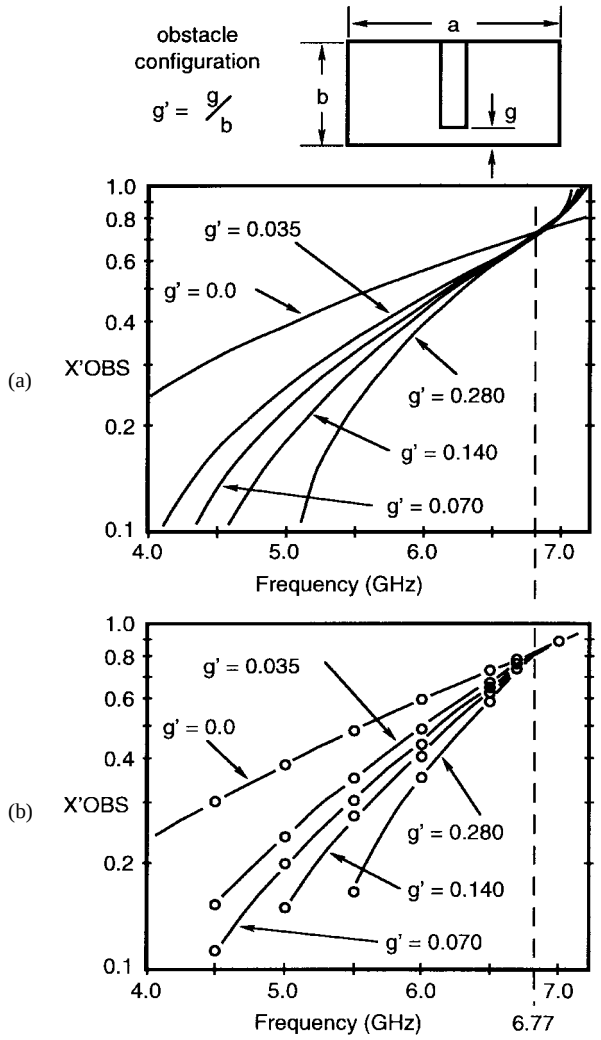

Fig. 10. Obstacle reactance for gap size "g" variation with $s' = 0.50$, $w' = 0.115$. (a) Theory. (b) Experiment.

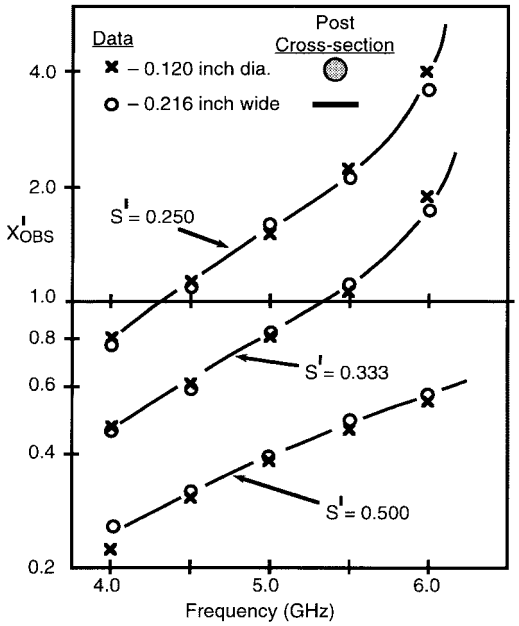

Fig. 11. Post cross-section comparison.

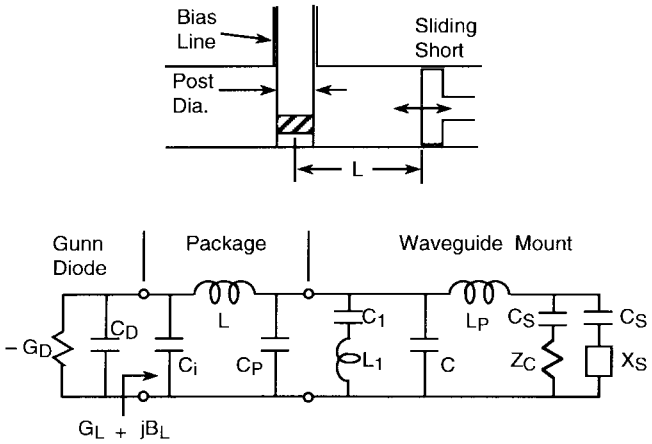

Fig. 12. Ku-band diode mount circuit.

reactance is independent of any impedance Z_G, which happens to be present at 6.77 GHz because the admittance function is infinite at this frequency due to the resonance of $C1$ and $L1$ shorting out the gap. This interesting feature would not be present if the gap were centered halfway up the post.

Electronically tunable elements can be designed using voltage-tunable devices mounted in this matter. By using reduced-height waveguide, the resonant frequency would be pushed higher, eliminating the restriction on the tuning curves. An example of such an element is the common switching element employing a p-i-n diode as a variable Z_G.

The second example shown here has the gap shorted (post from bottom to top,) thereby leaving only the post inductance (other examples are shown in [1]). Fig. 11 compares measurements for a circular post and flat post with the theory for the flat post for three different positions across the waveguide. This confirms that the approximation is justified for a flat post with a larger dimension representing a circular post.

VII. Gunn Oscillator Behavior

During the circuit development, several papers appeared that described unusual and unexplained tuning behavior of a Gunn diode in a waveguide mount with a sliding short. In some cases, the oscillation frequency was relatively insensitive to the tuning plunger position. In others, abrupt changes in frequency and power output were observed. These observations represented a ready-made opportunity to test the new equivalent circuit. The circuit model was extended to include the packaged diode and a tuning waveguide short circuit [8], as shown in Fig. 12.

Fig. 13 shows some frequency and power behavior predicted by the mount circuit, which closely resembles the published experimental results. Each curve in Fig. 13(a) is directly related to a frequency versus L tuning curve of the form in Fig. 14. Consider tuning the mount by increasing L, starting with $L \approx 0$. At some point the device starts to oscillate, with resulting output power. If the conductance associated with the tuning curve becomes greater than $|G_D|$, the oscillation at this frequency will cease. However, if another resonant condition exists, a new oscillation will be initiated at a reduced power level. This change-over will appear as

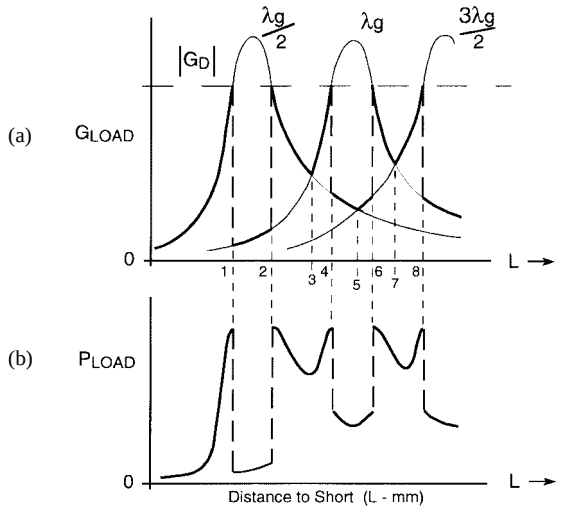

Fig. 13. Typical curves for a multiresonant waveguide mount.

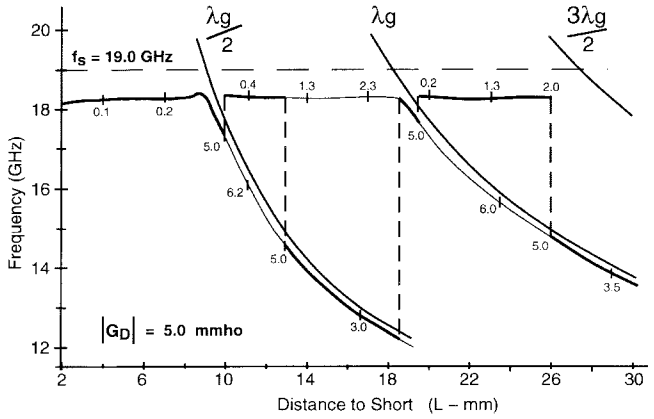

Fig. 14. Theoretical tuning curve showing frequency jumps.

a frequency and power jump and is indicated by the first discontinuity in Fig. 13 at point 1. As long as the $\lambda g/2$ curve remains above $|G_D|$, the tuning will follow the λg curve, as shown up to point 2. There transfer takes place back to the $\lambda g/2$ curve with the associated frequency and power jump. The next transition occurs at point 3, where it is observed that frequency jumps due to the curve transfer, but with a relatively constant power output due to continuity of G_L.

Fig. 14 shows the frequency variations for the tuning discussed. A "frequency saturation" effect is also shown here, whereby the tuning curves are limited at the high-frequency side by the 19-GHz boundary, established by the series resonance of elements $C1$ and $L1$ in the circuit. This is the same resonance noted in Fig. 10 and can be similarly increased by simply decreasing the guide height. This figure also shows the conductance values along the curves. Note that the tuning point leaves the curve when the conductance exceeds the maximum value for $G_D = 5.0$ mmho, jumping to the next available tuning condition. It also jumps back to the initial curve when the conductance drops back down below 5.0 mmho.

By using the "post in a waveguide" circuit, it was possible to fully explain the frequency tuning, jumping, and saturation along with output power variation and jumping that was being

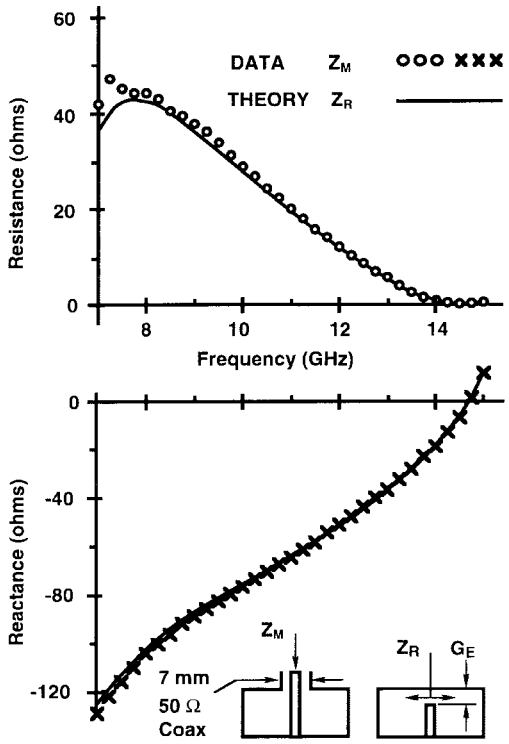

Fig. 15. Impedance comparison for equivalent gap versus coax.

reported by others in the literature. This "tuning characteristics" paper was referenced 17 times through the mid-1980's and was a strong contributor in convincing people of the power and utility of an accurate circuit model.

VIII. Coax-Gap Equivalence

It had been suspected for many years that a gap at the end of a post would have similar input impedance characteristics as a small coaxial entry with the post as the center conductor [6], [9]. Measurements were made and compared with the theory to determine if there was some sort of equivalence [10]. Fig. 15 shows a close correlation between the post gap [1] and a coaxial entry in the broadwall of a waveguide, measured in X-band waveguide.

It is concluded [10] based upon these measurements that the coax–waveguide junction can be represented by a post with a gap for nominal values of post and coax size. This then allows direct circuit design to be applied to configurations using the coax–waveguide junction.

IX. Extension to Two Gaps

Another very useful configuration that is related to the "post in a waveguide" is one with two gaps in the post [11]. Fig. 16 shows the versatility of this arrangement, and Fig. 17 shows the equivalent circuit.

This circuit has all of the same modes as before, but additional coupling mechanisms between the gaps and modes now exist in addition to the second gap. The same freedom to place the post position and the two gaps along the post is inherent in the circuit elements, and there is no restriction on the loading of the coaxial lines or the waveguide arms. The gap

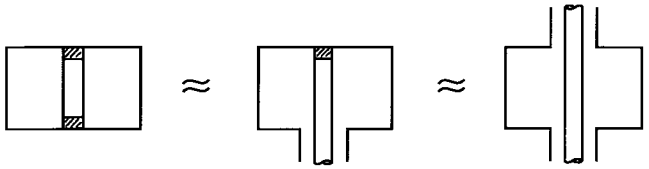

Fig. 16. Equivalent waveguide configurations for which the two-gap circuit can be applied.

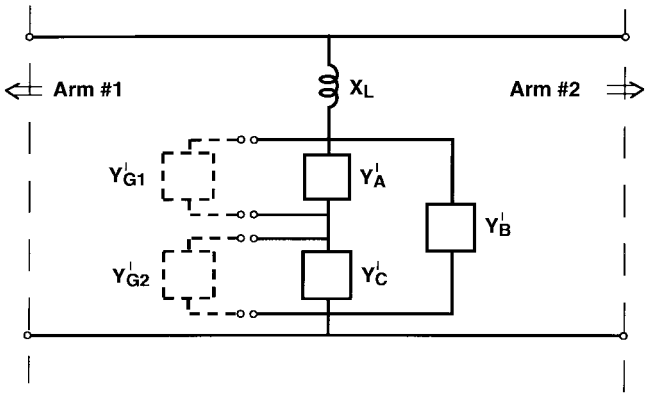

Fig. 17. Simplified two-gap circuit.

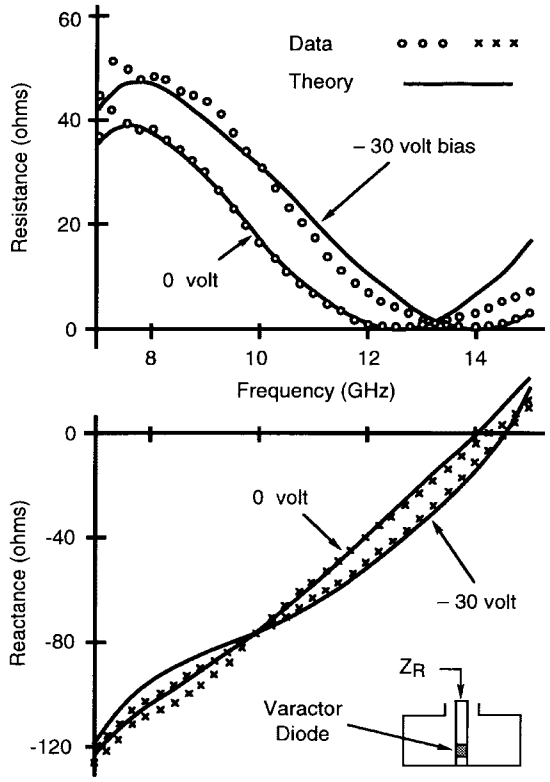

Fig. 18. Theory and experimental comparison for varactor tuning.

and coax configuration could represent a parametric amplifier or upconvertor, which has the appropriate filter in the coax line and a varactor in the gap. It could also be an IMPATT or Gunn oscillator with a sliding short in the waveguide, and using the coax to model the bias line with some loading, as demonstrated by Kurokawa.

Figs. 18 and 19 show a couple of additional comparisons of theory and experiment for variations of the two-gap configuration. Fig. 18 uses a standard packaged varactor in the gap with two different bias conditions to show the effect of changing the capacitance in the gap. Surprisingly, there is more shift in the resistance than in the reactance. Nominal values for the varactor and its package elements were used, thus, some of the deviation from theory could be due to error in these values. Fig. 19 addresses the double coax configuration with a varying load on the opposite coax port. One case has a 50-Ω termination and the others are two positions of a sliding short to simulate large changes in reactance.

The correlation is not perfect in these comparisons using coax, but quite usable considering all of the approximations or "equivalencies" involved. Certainly, the theory is accurate enough to do initial designs before fine tuning.

X. Contributions by Others

As the years have passed, application of these theoretical and measurement techniques have not diminished as use of waveguide circuits have shifted to higher frequencies. The rest of this paper focuses on the works of others, who used the analysis/measurement technique to do something new or extended the analysis to a different application. Some of the more unique or interesting papers of over 100 appearing since 1971, are briefly discussed, more or less in chronological order.

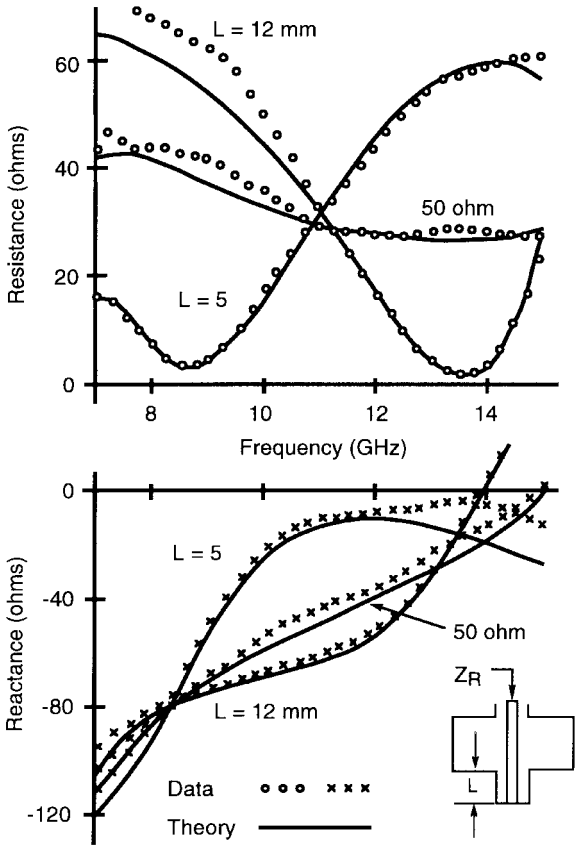

Fig. 19. Theory and experimental comparison for a load and sliding short.

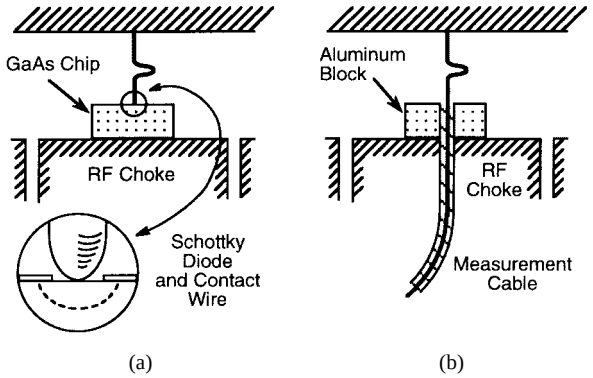

Fig. 20. Model for embedding impedance measurement. (a) Actual configuration. (b) Scaled model with cable.

Jethwa and Gunshor used the equivalent circuit to explain tuning and mode jumping effects for a Gunn diode oscillator [12]. This parallels the results of [8].

Williamson published many papers for a variety of waveguide mounts and takes into account the cylindrical nature of the post. The first of these [13] shows results only, comparing to measured data of [1]. A full analysis is made later in [14].

El-Sayed had the first paper to apply the analysis to two flat posts in the same waveguide cross section [15].

Next is a discussion of five papers by Kerr, either as author or co-author, demonstrating improvement in mixer performance. The first is a landmark paper in low-noise millimeter-wave receivers [16]. It is the first time cryogenically cooled Schottky mixers were used, and the noise temperature was about half that of the previous state-of-the-art. The use of [1] was to provide an understanding of the waveguide mount to the author so that the design would allow the diode to see an acceptable impedance over the whole waveguide band. Previously, attempts had been limited to cases in which the diode had a fairly simple embedding network. The second paper was selected for the 1978 Microwave Prize [17]. This was the first accurate analysis of a Schottky diode mixer, taking into account harmonic terminations up to 6fLO. This paper used the experimental technique on a 64× scale model so that the embedding impedance for a greater than 6:1 frequency range could be characterized. Fig. 20 shows how the cable replaced the Schottky diode to make these measurements. The third paper demonstrated for the first time the accuracy of Tucker's three frequency quantum mixer theory using an SIS mixer with a fairly large ωRC product [18]. This paper used the experimental technique on a 40× scale model so that the embedding impedance could be accurately measured. The fourth paper also used the measurement technique [19], this time on a 100× scale model over 6fLO. The fifth paper was the first 100-GHz mixer to come close to the fundamental quantum noise limit with $T_{\text{mixer}} < 5.6$ K, nonclassical conversion loss [$L = 0$ dB double sideband (DSB)], and negative IF output resistance (in a resistive mixer) [20]. In this paper, the form of the equivalent circuit is based upon [1], from which it was possible to identify the circuit reactances with energy storage in particular groups of evanescent waveguide modes. This choice of equivalent circuit results in elements that are not strongly frequency dependent, and allows a more intuitive understanding of the mount. Actual values were measured using a 40× scale model.

Alexander and Khan applied the analysis to a coaxial cavity with a gap in the center conductor [21].

Joshi performed a major extension of the analysis in 1977 with a pair of papers, characterizing the circuit to allow multiple semiconductor devices to be included and, subsequently, a development that allowed multiple posts with different devices in the gaps [22]. The first of the pair provided a more general extension to multiple gaps, allowing them to be either in the same post or separate posts. The second paper then discussed in detail the cases of two gaps. The two-post configuration allows much more flexibility in circuit design and has been applied successfully to varactor-controlled oscillator circuits. Such an application was not feasible with the two gaps in a single post because of the need for independent biasing of the varactor and source diodes. Application of this work led to a large program at Philips Broadband Networks supplying varactor-tuned Gunn oscillators for the Skyflash air-to-air missile over several years.

Eaton and Joshi followed with an excellent applications write-up for the two-post configuration [23], which discusses many options with the posts, gaps, and other parameters involved, leading to the successful design of commercial products.

Mizushina *et al.* applied the basic analysis to a ridged-waveguide configuration, resulting in wider bandwidth operation for the mount [24].

Here is another group of three papers with an interesting similar extension of the analysis. Rutledge and Schwarz demonstrated the flexibility of the analysis approach for active structures (detector and oscillator grids) [25] when it was determined that if free-space modes were substituted for the formulation, then the impedance for these structures could also be predicted with excellent agreement between theory and experiment. This was particularly interesting because there is no waveguide. Popović *et al.* represents another extension, this time to a two-dimensional grid loaded with transistors, placed inside a Fabry–Perot cavity, and demonstrating a quasi-optical approach for generation of microwave power [26]. The grid acts as an active surface with a reflection coefficient greater than unity, allowing oscillations to build up. Assuming an infinite array of devices and a plane-wave excitation, an equivalent waveguide unit cell is defined for a parallel-plate waveguide, having electric walls on the top and bottom and magnetic walls on the sides. An equivalent circuit can then be developed for this configuration, adapting for the modified waveguide. Popović *et al.* then used a similar approach to the "bar-grid" paper, with a modified configuration, this time supporting 100-MESFET's on a substrate [27]. Fig. 21 is a photo of the 100-element planar array. Biasing lines are connected to the sides of the array. Fig. 22 is a closer view of the connections to the individual MESFET's and it shows the symmetry for defining the unit cell. All of the devices share the same biasing and tuning circuit, making the structure attractive for combining a very large number of devices. This paper was also awarded the Microwave Prize.

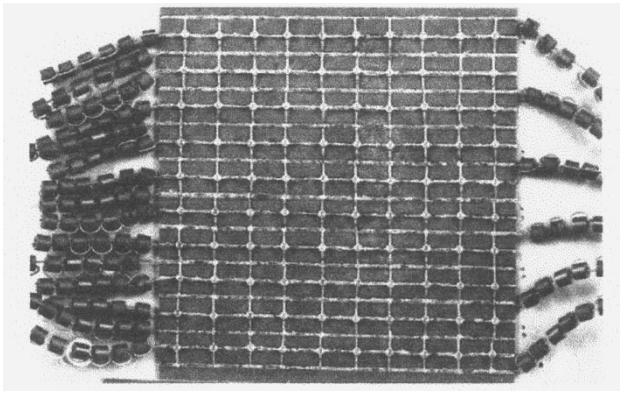

Fig. 21. 100-MESFET array.

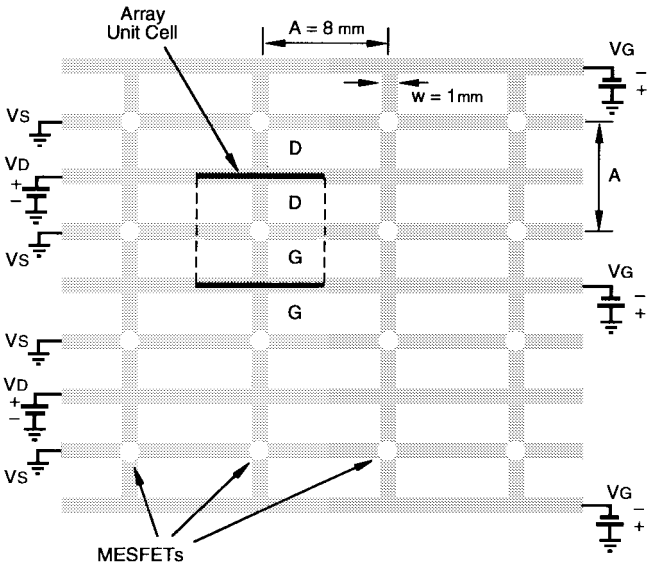

Fig. 22. Biasing arrangement for the array unit cell.

Hicks and Khan investigated the equivalence ratio between round and flat posts by taking into account the current variation across the post [28]. Curves are provided, showing the dependence on post diameter, post position, and frequency.

Skrehot and Chang used the equivalent circuit for the two-gap configuration in a novel way to characterize the material of the flat post [29]. The calculated resonant frequencies and normalized surface resistance agree well with the measurements over a frequency range of 8–18 GHz.

Bates and Ko used the measurement technique once again to confirm an analysis for a complicated circuit, this time having very irregular radial resonant elements [30].

XI. Conclusion

This paper has presented an overview of the contribution of the paper upon which the 1999 Microwave Pioneer Award was based. The subject paper provided a theoretical solution of the general problem of the circuit impedance seen by a device mounted in shunt across a waveguide. The resulting equivalent circuit can be used to improve the design of waveguide oscillators, amplifiers, frequency multipliers and converters, phase shifters, mixers, attenuators, and various filter elements. A validating measurement technique was presented. A variety of applications of the analysis and measurements were discussed, including the related works of others.

Acknowledgment

This paper was previously published in the *IEEE Microwave Theory and Techniques Newsletter*, no. 151, Spring 1999, and is published here for archiving purposes due to its tutorial and reference value.

References

[1] R. L. Eisenhart and P. J. Khan, "Theoretical and experimental analysis of a waveguide mounting structure," *IEEE Trans. Microwave Theory Tech.*, vol. MTT-19, pp. 706-719, Aug. 1971.
[2] W. J. Getsinger, "The packaged and mounted diode as a microwave circuit," *IEEE Trans. Microwave Theory Tech.*, vol. MTT-14, pp. 58–59, Feb. 1966.
[3] ———, "Mounted diode equivalent circuits," *IEEE Trans. Microwave Theory Tech.* vol. MTT-15, pp. 650–651, Nov. 1967.
[4] E. Yamashita and J. R. Baird, "Theory of a tunnel diode oscillator in a microwave structure," *Proc. IEEE*, vol. 54, pp. 606–611, Apr. 1966.
[5] P. S. Carter, "Circuit relations in radiating systems and applications to antenna problems," *Proc. IRE*, vol. 20, pp. 1004–1041, June 1932.
[6] R. E. Collin, *Field Theory of Guided Waves*. New York: McGraw-Hill, 1960.
[7] R. L. Eisenhart, "Impedance characterization of a waveguide microwave circuit," U.S. Army Electron. Command, Fort Monmouth, NJ, Tech. Rep. 208, 1971.
[8] R. L. Eisenhart and P. J. Khan, "Some tuning characteristics and oscillation conditions of a waveguide-mounted transferred-electron diode oscillator," *IEEE Trans. Electron Devices*, vol. ED-19, pp. 1050–1055, Sept. 1972.
[9] L. Lewin, "A contribution to the theory of probes in waveguides," *Proc. Inst. Elect. Eng.*, pp. 109–116, Oct. 1957.
[10] R. L. Eisenhart, P. T. Greiling, L. K. Roberts, and R. S. Robertson, "A useful equivalence for a coaxial-waveguide junction," *IEEE Trans. Microwave Theory Tech.*, vol. MTT-26, pp. 172–174, Mar. 1978.
[11] R. L. Eisenhart, "Discussion of a 2-gap waveguide mount," *IEEE Trans. Microwave Theory Tech.*, vol. MTT-24, pp. 987–990, Dec. 1976.

Other Contributions

[12] C. P. Jethwa and R. L. Gunshor, "An analytical equivalent circuit representation for waveguide-mounted Gunn oscillators," *IEEE Trans. Microwave Theory Tech.*, vol. 20, pp. 565–572, Sept. 1972.
[13] A. G. Williamson and D. V. Otto, "Analysis of a waveguide mounting structure," in *Proc. IREE Aust.*, Apr. 1973, pp. 95–97.
[14] A. G. Williamson, "Analysis and modeling of a single-post waveguide mounting structure," *Proc. Inst. Elect. Eng.*, vol. 129, pt. H, no. 5, pp. 271–277, Oct. 1982.
[15] O. L. El-Sayed, "Impedance characterization of a two-post mounting structure for varactor-tuned Gunn oscillators," *IEEE Trans. Microwave Theory Tech.*, vol. MTT-22, pp. 769–776, Aug. 1974.
[16] A. R. Kerr, "Low-noise room-temperature and cryogenic mixers of 80–120 GHz," *IEEE Trans. Microwave Theory Tech.*, vol. MTT-23, pp. 781–787, Oct. 1975.
[17] D. N. Held and A. R. Kerr, "Conversion loss and noise of microwave and millimeter-wave mixers: Part 2—Experiment," *IEEE Trans. Microwave Theory Tech.*, vol. MTT-26, pp. 55–61, Feb. 1978.
[18] M. J. Feldman *et al.*, "SIS mixer analysis using a scale model," *IEEE Trans. Magn.*, vol. MAG-19, pp. 494–497, May 1983.
[19] P. H. Siegel and A. R. Kerr, "The measured and computed performance of a 140–220-GHz Schottky diode mixer," *IEEE Trans. Microwave Theory Tech.*, vol. MTT-32, pp. 1579–1590, Dec. 1984.
[20] S. K. Pan *et al.*, "An 85–116-GHz SIS receiver using inductively shunted edge junctions," *IEEE Trans. Microwave Theory Tech.*, vol. 37, pp. 580–592, Mar. 1989.
[21] P. H. Alexander and P. J. Khan, "Wide-band characteristics of a coaxial-cavity solid-state device mount," *IEEE Trans. Microwave Theory Tech.*, vol. MTT-23, pp. 831–833, Oct. 1975.
[22] J. Joshi and J. A. F. Cornick, "Analysis of waveguide post configurations: Part I—Gap immittance matrices: Part II—Dual-gap cases," *IEEE Trans. Microwave Theory Tech.*, vol. MTT-25, pp. 169–181, Mar. 1977.

[23] R. M. Eaton and J. S. Joshi, "Design VCO's accurately with computer analysis," *Microwaves*, pp. 70–80, July 1977.
[24] S. Mizushina *et al.*, "Theoretical analysis of a ridged-waveguide mounting structure," *IEEE Trans. Microwave Theory Tech.*, vol. MTT-25, pp. 1131–1134, Dec. 1977.
[25] D. B. Rutledge and S. E. Schwarz, "Planar multimode detector arrays for infrared and millimeter applications," *IEEE J. Quantum Electron.*, vol. QE-17, pp. 407–414, Mar. 1981.
[26] Z. B. Popović *et al.*, "Bar-grid oscillators," *IEEE Trans. Microwave Theory Tech.*, vol. 38, pp. 225–230, Mar. 1990.
[27] ——, "A 100-MESFET planar grid oscillator," *IEEE Trans. Microwave Theory Tech.*, vol. 39, pp. 193–200, Feb. 1991.
[28] R. G. Hicks and P. J. Khan, "Improved waveguide diode mount circuit model using post equivalence factor analysis," *IEEE Trans. Microwave Theory Tech.*, vol. MTT-30, pp. 1914–1920, Nov. 1982.
[29] M. K. Skrehot and K. Chang, "A new resistance measurement technique applicable to high-temperature super-conducting materials at microwave frequencies," *IEEE Trans. Microwave Theory Tech.*, vol. 38, pp. 434–437, Apr. 1990.
[30] B. D. Bates and A. Ko, "Modal analysis of radial-resonator waveguide diode mounts," *IEEE Trans. Microwave Theory Tech.*, vol. 38, pp. 1037–1045, Aug. 1990.

Robert L. Eisenhart (S'70–M'70–SM'92–F'95), for photograph and biography, see this issue, p. 2181.